JOURNAL OF APPLIED POLYMER SCIENCE VOL. VI, ISSUE NO. 21, PAGES 338-351 (1962)

Behavior of High Strength Parachute Components at Impact Velocities up to 700 Feet per Second

ROBERT J. COSKREN, HENRY M. MORGAN, and CHAUNCEY C. CHU

Fabric Research Laboratories, Inc., Dedham, Massachusetts

INTRODUCTION

One of the common areas in which little effort has been expended in the past is the impact studies at high rates of loading of textile materials. Today, in an air age of supersonic speed aircraft, missile systems, and the advent of space vehicles a need for impact behavior data of textiles definitely exists. Evidence of this need is shown through several reports which have indicated that rupture or failure of parachute suspension lines has occurred during high speed tests of first stage recovery parachute systems. The data recorded revealed that failure of the suspension lines occurred although the total load was less than 50% of the total rated strength of the lines. These problems have steadily increased in number and complexity. Requirements for recovery missiles involve speeds up to Mach 3, flight altitudes of 500,000 ft., and weights up to 10,000 lb.

Part of the parachute design is concerned with the fabrication of various seams, splices, and joints. These various configurations, commonly called overlap splices, skirt band joints, vent band joints, butterfly gusset, and felled seams are also subjected to impact conditions together with the webbings and suspension lines. In order to evaluate the response of such systems to impact loading conditions a new test instrument was required. A contract was awarded to Fabric Research Laboratories, Inc., by the Aeronautical Systems Division of the U.S. Air Force to develop and use such a machine.

One of the objectives of the research was to design and construct an impact test machine capable of rupturing specimens with static strengths of up to 10,000 lb. at impact velocities ranging from 200 to 750 ft./sec., which is considerably in excess of 500,000 in./min.; the breaking of the specimens at these velocities, however, is only secondary in importance to the collection of other physical data such as: load/elongation versus time curves, times to rupture, impact velocities, and rupture energies, which were heretofore difficult if not impossible to obtain from other methods.

GENERAL CONSIDERATIONS OF SYSTEM DESIGN

Impact testing at high rates of loading differs from static testing primarily from the essential consideration of the phenomenon of stress wave propagation in both the test specimen and the attachments. In static testing, the force applied to extend the specimen is uniform throughout the entire length of the test piece. At impact velocities there is a nonuniform increase in load which is a consequence of the stress wave; i.e., the applied force on one end of the specimen is not instantly measurable from the restrained or the clamped end. Failure to consider this phenomenon can lead to the use of force gages with inadequate frequency response characteristics.

In textile materials, this stress wave phenomenon manifests itself at impact velocities in excess of 100 ft./sec. The resistance offered by the internal inertia of the specimen to an applied impact produces stress waves which are reflected from end to end until the breaking stress of the specimen is reached. The fronts of these stress waves are step functions with rise times in the order of from 1 to 10 μsec. Thus, a true measure of the force in a specimen at any time requires the use of a force gage with a resonant frequency of upwards of one megacycle ($f = 1/T$). Such gages are not currently available.

If stress waves are not considered, calculations can be made to show that a load cell with a resonant frequency in the range of 25 to 50 kc. might suffice. Unfortunately, such load cells cannot give the stepwise force-time behavior which actually occurs.

The reason for discussing the stress waves and load cell design is that the system of rupturing the test specimens employed was tailored to the only

measuring system known to be successful in obtaining useful data. It is, in fact, the *measuring system* which must be considered of paramount importance since it is the source of the desired information.

The Measuring System

In view of the foregoing discussion, load cells using either strain gages or piezoelectric transducers either directly or as accelerometers (i.e., the principle of inducing reaction forces in a secondary system) were rejected because of their inadequacy to respond to the load rise times encountered. The system which is best suited for this problem is one which measures the impact force by the deceleration of a known impacting mass by the use of a high speed photographic technique described below. Rather than use high speed motion picture cameras of up to 25,000 frames/sec. which are expensive and difficult to operate and process, a multimicroflash technique is used. Separate ultra-high speed flashes spaced at given time intervals "stop" the motion of the test specimen as well as the impacting mass. These "stopped" motions are caught on a large (4 x 5 in.) photographic film as a multiple exposure.

Edgerton, Germeshausen and Grier, Inc., of Boston, designed and built a multimicroflash unit especially for the study. This unit, plus a standard open-shutter camera, provides sufficient data for the calculation of: (*a*) impact force as a function of time, (*b*) specimen extension, (*c*) effective gage length, and (*d*) energy to rupture.

The deceleration as measured by double differentiation of specimen displacement in the photographic record is cross checked by the use of two ballistic pendulums. The displacement of the first pendulum, which also contains the specimen holder, gives a measure of the impulse delivered to the specimen. The impulse is defined by the integral of the force-time function and is measured by the change in momentum of the pendulum. The second pendulum catches the impacting mass after it ruptures the test specimen. The motion of the second pendulum is proportional to the residual momentum of the impacting mass. From the momentum, before and after impact, the energy lost by the impacting mass is calculated and checked against the energy absorbed by the specimen calculated by the photographic method.

The Impacting System

The impacting system, as mentioned previously, consists essentially of a free moving impacting mass whose deceleration is measured. Alternative impacting devices have been considered and rejected for a variety of reasons. Some examples are as follows:

1. Rotating systems seem plausibly attractive since it is thereby possible to get controlled velocities. Impact machines using rotating impact heads have been used at the National Bureau of Standards and Wright Air Development Division, as well as at Fabric Research Laboratories, Inc. However, in all these cases, impact speeds are well below 750 ft./sec., and impact forces well below 10,000 lb. At high speeds and high energy requirements, a rotary system was considered impractical for two reasons: (*a*) the potential hazards associated with rotary inertia, particularly when unbalanced forces are applied at impact, and (*b*) the long time required to accelerate and decelerate the heavy flywheels.

2. Mechanical systems such as stretched springs have been ruled out because it is not possible to get the required velocities by this means directly. The reason is that the inertia of the springs themselves restricts their motion and limits the ultimate velocity obtainable. It is true that a small mass could achieve a high velocity if it is first impacted by a large slower moving mass. However, a secondary missile system of this type was not considered practical.

3. Gravity systems are naturally out of the question since the required heights are much too great and terminal velocities of much less than 750 ft./sec. will be reached.

4. Hydraulic systems are even less feasible than the mechanical spring system since the mass of the piston involved creates similar, if not more severe, inertial problems.

Thus the system of the freely moving impacting mass is the only feasible approach, wherein compressed gas is used to accelerate the mass and the deceleration of the mass is the primary means of measurement. The mass and/or velocity of the missile can be varied according to the requirements of the specimen and test.

The Specimen Holders

The clamping of textile specimens in tensile testing is a notoriously difficult problem. Capstan-type grips are normally used when high strength webbings are tested. In spite of the difficulties produced by such grips, such as the determination of the effective gage length, they represent the most satisfactory clamp system known. However, the

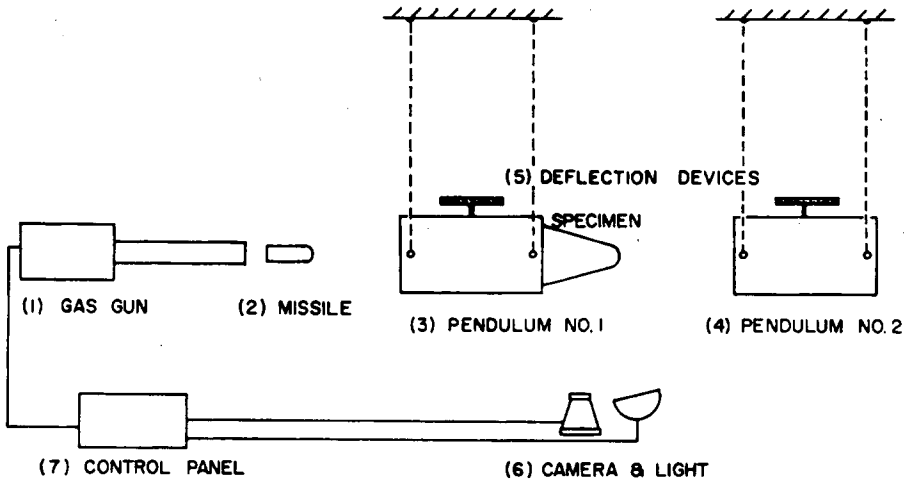

Fig. 1. Schematic diagram of impact testing machine.

mass of the capstan grips necessary to hold webbings with 10,000 lb. breaking strength is considerable. If the impacting system which has been described in the previous section were to include the mass of a capstan grip of this type, the thrust required to reach the desired velocities would be unusually large. A V-shaped specimen configuration has therefore been adopted where the impacting mass will strike the specimen at the apex of the V while the two ends of the V are clamped in capstan grips mounted on the first ballistic pendulum.

DESIGN OF THE IMPACT TEST MACHINE

Figure 1 is a schematic diagram showing the major components of the impact test machine. It consists of the following: (*1*) the gas gun or the impacting mass launcher, (*2*) the missile or the impacting mass, (*3*) ballistic pendulum No. 1 with specimen holders, (*4*) ballistic pendulum No. 2, (*5*) pendulum deflection indicating devices, (*6*) camera and the multimicroflash light source, and (*7*) control panel.

Figure 2 is a photograph of the entire machine. The design, function and operation of each of the above items is given below. Figure 3 shows a sample mounted on the rear of the first pendulum.

The Gas Gun

Design Requirements

Since the primary function of the gas gun is to launch the impacting mass and propel it at the desired velocity with sufficient energy to rupture the various specimens, the design has to be tailored to the elastic properties of the materials to be tested and their physical configurations. These are: (*1*) velocity range—200 to 750 ft./sec.; (*2*) spec-

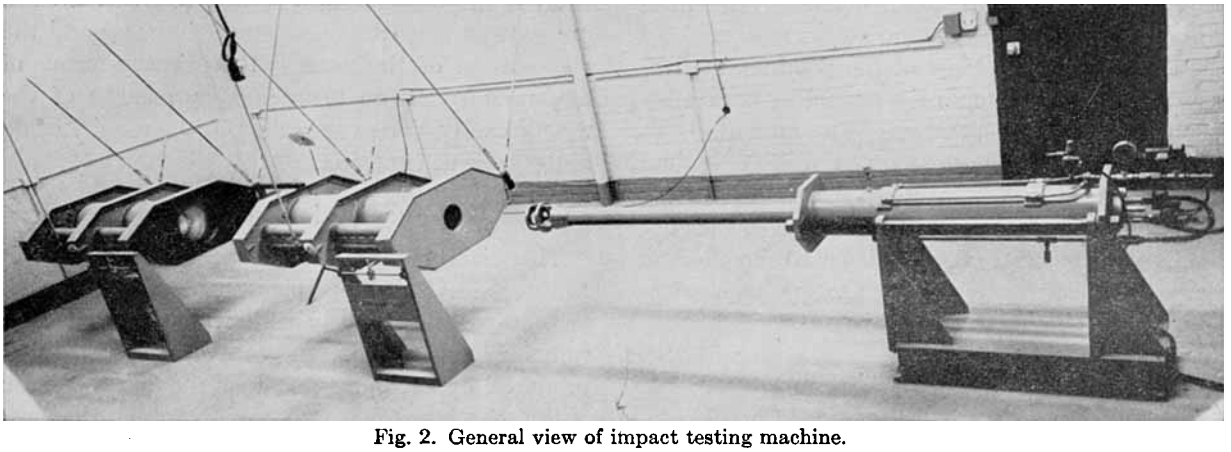

Fig. 2. General view of impact testing machine.

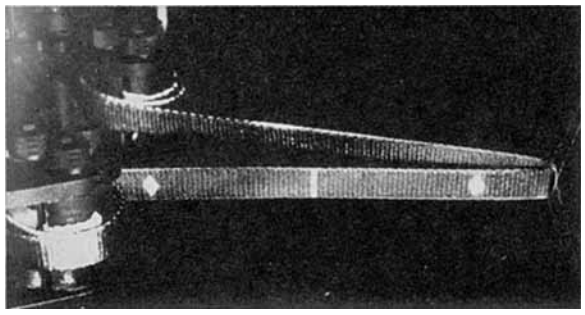

Fig. 3. Specimen mounted on rear of first pendulum.

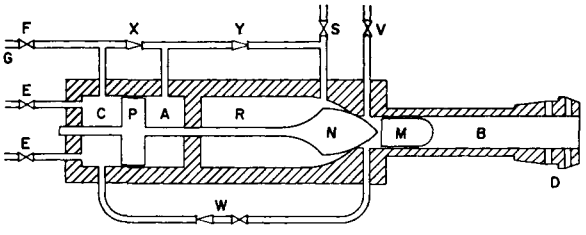

Fig. 4. Schematic diagram of gas gun.

imen width—up to 2 in. (webbings); and (*3*) elastic properties of test specimens: (*a*) static breaking strength—up to 10,000 lb., (*b*) effective gage length —up to 48 in., (*c*) specimen extension—up to 25%.

Figure 4 is a schematic diagram of the gas gun which functions as follows.

1. Gas at a predetermined pressure enters feed hose G through solenoid operated valve F (normally closed) and check valves X and Y to fill the three different compartments C, A, and R of the gun.

2. Piston P and the valve needle N which are mounted on a common shaft keep the gas in the receiving chamber R from escaping into the barrel B.

3. Vent valve V is solenoid operated and is normally open to allow any leaking gas to escape without the danger of accidentally firing the missile M and is closed when the gun is fired. The safety valve S prevents overcharging.

4. When the gun is ready to be fired, either one or both of the solenoid operated exhaust valves E are opened, allowing gas in chamber C to escape. When this occurs, the pressure in chamber A is greater than the pressure in chamber C creating pressure differential on the two surfaces of piston P which moves the piston toward the left and simultaneously withdraws the needle N from its seat.

5. The gas in the receiving chamber R now rushes through the opening between the needle N and its seat thus forcing the missile M down the barrel B.

6. Part of this escaping gas is piped through a

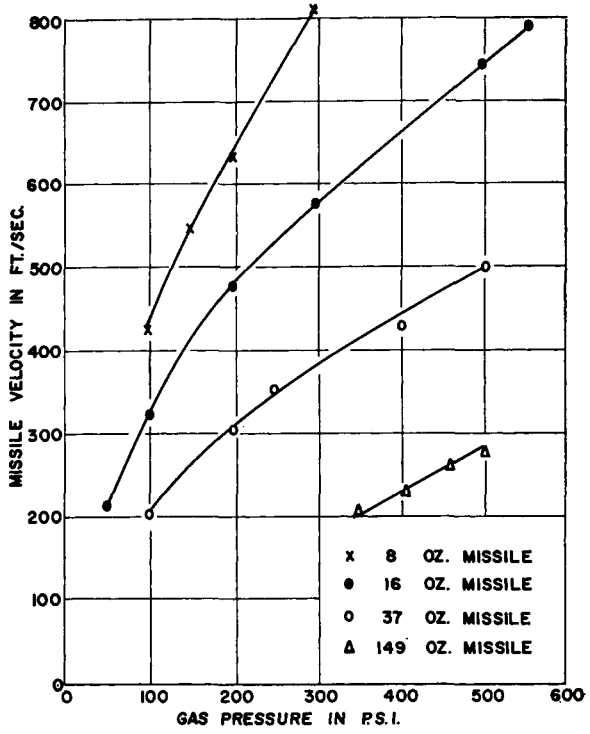

Fig. 5. Pressure versus velocity for various missiles (helium gas).

flow and check valve W to chamber C to rebuild its lost pressure thereby cushioning the piston P and preventing it from slamming against the end of the chamber.

7. The gas, both in front and behind the missile M, is permitted to diffuse through the openings in the diffuser D to minimize the effect of the gas blast which may introduce erroneous readings on the pendulums.

Dimensions and Capacities

The gun is approximately 10 ft. long with a bore of 2.5 in. and a barrel length of 5 ft. Both the gas-receiving chamber and the barrel were designed for a maximum working pressure of 5000 psi* with a factor of safety of 5.

The volume of the gas receiver (chamber R, Fig. 3) is approximately 600 cu. in. which is adequate to propel missiles of up to 10 pounds in weight at velocities up to 800 ft./sec. using gas pressures of well below 1000 psi. A calibration curve of helium pressure versus velocity for various missiles is shown in Figure 5.

* Based on the Lame equations, pp. 5–65, *Marks' Mechanical Engineers' Handbook*, T. Baumeister, Ed., 6th ed., McGraw-Hill, New York, 1958.

The Missile

Mass of the Missile

For evaluation of the specimens under study it has been calculated that four missiles of varying masses are required. Combinations of mass and velocity may be selected to supply the anticipated energy for rupturing a given specimen. Figure 6 shows the shapes and relative sizes of four missiles used. The missiles used are: (*a*) 8 oz., (*b*) 16 oz., (*c*) 40 oz., and (*d*) 160 oz.

Configuration of the Missile

The missile is cylindrical in shape with the nose machined in the form of a half cylinder whose axis is perpendicular to the axis of the missile. Upon impact, the cylindrical shaped nose fits into the curved portion of the V-shaped specimen.

Each missile consists of four parts which are:

1. The nose or the impacting surface which is machined from linen-inserted phenolic plastic selected for its superior impact properties.

2. The body of the missile is a length of cylindrical material whose function is to provide mass. It can be solid or tubular and may be made of either metal or plastic, depending on the mass required.

3. The sabot or tail piece which is again made of linen-inserted plastic.

4. Teflon seal/bearings in the form of two O-rings are used between each of the three pieces mentioned above with the shortest and lightest missile. These rings provide low friction bearing surfaces for the missile to slide on and also seal against gas leakage. Only one O-ring is used on the larger missiles. In addition, Teflon runners are used along the body of the longer and heavier missiles to provide the low friction-bearing surfaces.

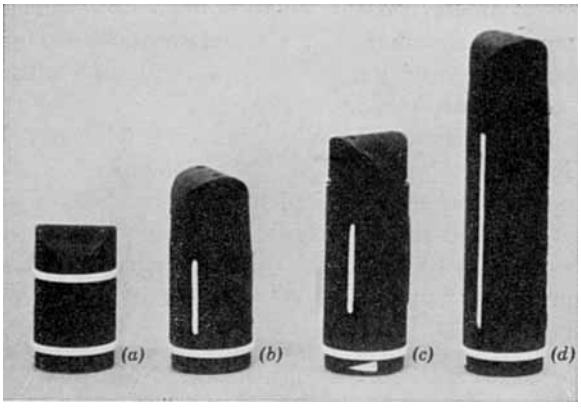

Fig. 6. Four impacting masses.

The Ballistic Pendulum

Function

The first ballistic pendulum is used primarily as a low frequency specimen mounting device. Additionally, if the mass is known and its displacement after impact is measured, the velocity and the energy of the missile can be calculated according to the equation of momentum transfer:

$$M_1 \Delta V_1 = M_2 V_2 \tag{1}$$

where M_1 is the mass of the missile, M_2 the mass of the first pendulum, ΔV_1 the change in velocity of the missile, V_2 the velocity of the pendulum after impact, and the V_2 can be expressed as

$$V_2 = dx/dt = 2\pi/T(D \cos 2\pi t/T) \tag{2}$$

where dx/dt is the horizontal velocity of the pendulum, D the displacement of the pendulum, T the period of the pendulum, and t the time after impact.

However, at the moment of impact, $t = 0$.

Hence,

$$\cos 2\pi t/T = 1 \tag{3}$$

then

$$V_2 = 2\pi D/T \tag{4}$$

Combining eqs. (1) and (4):

$$\Delta V_1 = 2\pi\, DM_2/TM_1$$

where V_3 is the residual missile velocity after the sample has ruptured.

After calculating the residual velocity of the missile from the displacement of the second pendulum it is possible to calculate the initial velocity V_1 from above. The calculated velocity may also be checked from the photographic record of the test. Knowing the initial and residual missile velocities it is possible to calculate the energy absorbed by the specimen from

$$E = {}^1/_2 M\,(V_1^2 - V_3^2)$$

where V_3 is the residual missile velocity after the sample has ruptured.

The second pendulum also serves a dual purpose. It is first a means for measuring, by its displacement, the velocity and the residual energy in the missile after rupturing the test specimen. And secondly, it is a low frequency shock mount for stopping and containing the missile after each test. Here again the mass is variable depending upon the mass and the velocity of the missile.

Configuration of the Pendulums

Referring to Figure 2, it is seen that the pendulums are fabricated from welded aluminum components. In the center is the body of the pendulum made of a length of 12 in. pipe through which the missile passes. On either side are two rails on which cast iron augmenting weights may be added to increase the mass of the pendulum. The augmenting weights are so designed as to maintain the center of percussion of the pendulum regardless of the number of weights added. Spaced evenly are three bulkheads whose purpose is to provide support for the aforementioned rails and attachments for the pendulum suspension system.

Photographic System

The equipment used to record the impact data consists chiefly of the multiflash light source and a 4 x 5 view camera.

Multiflash Unit

The multiflash unit makes use of 15 separate energy storing circuits (discharge units) and produces 15 pulses of light each with a duration of about 1 μsec., an energy per flash of 1.5 w.-sec., and a time interval variable from 10 μsec. to 10 msec. between flashes. A multiple exposure photograph of a missile in flight is shown in Figure 7.

Camera

The camera used in conjunction with the multiflash unit need be of the simplest design. The only basic requirement is that the camera lens be of sufficiently good quality in order to insure getting a properly exposed and focused negative.

The impact photographs are taken in a darkened room using only the light emitted by the multiflash flashtube. The camera shutter is used on its "time" setting which means it is opened manually a few seconds before the multiflash is triggered and closed a few seconds after the test is completed. There is no need for synchronizing the opening of the shutter with the triggering of the light since very little film "fogging" occurs from over-exposure in the darkened room.

With regard to film, it is essential that a high emulsion speed film be used with the multiflash. The duration of the light (1 μsec.) and its resulting intensity is such that maximum film speed is essential. Films which have been used in increasing order of satisfaction include Eastman Kodak

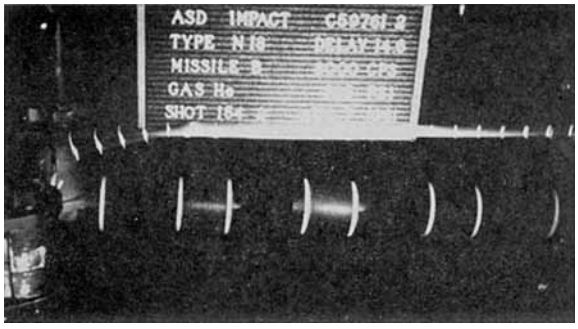

Fig. 7. Multiple exposure of missile in flight.

Tri-X, Superpanchro Press-type B, Royal Pan, and Royal-X-Pan. Also investigated were Ansco's Hypan and Super Hypan. Kodak's Royal-X-Pan has proven most satisfactory for the impact work because of its combination of high emulsion speed and moderate "grain" level. A Polaroid camera is used in addition to the 4 x 5 standard camera thus making it possible to make rapid judgments as to the need for processing negatives in the darkroom.

CALCULATIONS AND DATA ANALYSIS

As mentioned earlier, the uniqueness of the present impacting system is primarily in the use of photographic techniques for compilation of data. From the photograph of the specimen during impact it is possible to measure and calculate the following parameters: (*a*) force to rupture the specimen, (*b*) specimen extension at rupture, (*c*) force-extension diagram, (*d*) force and/or extension time curve, and (*e*) work to cause rupture.

It is also possible to measure missile velocity before, during, and after impact as well as to measure the effective gage length of the specimen involved in any given test. A detailed description of the various techniques employed to determine the aforementioned variables follows below.

Force to Rupture the Specimen

The most common way of measuring the tensile force imposed on a textile material loaded longitudinally on a tensile testing machine is with an electronic strain gage system. Unfortunately, when a material is strained at a high rate the conventional strain gage setup is unable to respond i.e., the rate of loading is so rapid that the specimen rupture load builds up more rapidly than can be detected by the gage. Hence, the need for a more sensitive system.

In the current program the photographic technique was decided upon for several reasons. In

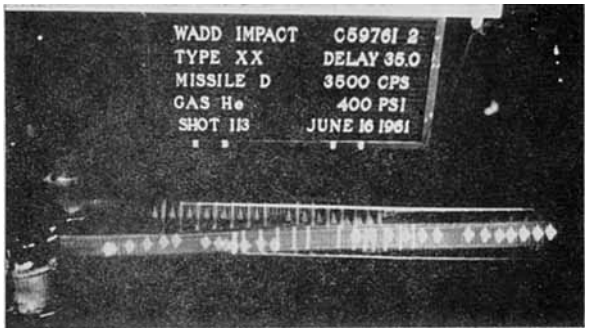

Fig. 8. Typical photograph of impact test.

the first place, as mentioned above, there is considerable danger in selecting a mechanical or electrical strain-gage system which may be only partly responsible. Electronic devices, such as accelerometers, could be used. However, the frequency response of such systems can cause trouble due to the large masses of the sample grips. Another reason for using the photographic method is that it supplies other useful information on the behavior of the specimen before, during, and after loading. The multiple exposure film gives a permanent record of each test. Figure 8 is an actual impact photo, and Figure 9 is a schematic representation of the important parts of the photo.

The measurement of rupture force is accomplished by measuring the deceleration of the missile as it ruptures the specimen. It is known that

$$F = ma$$

where F is the rupture force, m the mass of projectile, and a the deceleration of projectile.

The spacing between successive exposures of the missile as it impacts the specimen can be accurately measured on the enlarged photographic print. The time between light flashes is controlled by the multiflash unit. Knowing these distances and times it is possible to calculate the missile velocity at any given instant. The velocity *change* indicates deceleration. The mass of the projectile times the deceleration is the force supplied by the test sample acting on the projectile.

Rupture Extension

The rupture extension is measured directly from the photograph of the specimen during impact. Initially two gage marks are placed at a known interval on that leg of the sample which faces the camera. As the sample is strained during impact the distance between the gage marks increases on successive exposures by the multiflash. The extension at rupture as well as at various times prior to rupture can thereby be measured.

Force and/or Extension-Time Diagram

Since the time between successive exposures can be accurately determined from the multiflash, the force and/or extension-time relationship can be determined.

Rupture Energy

The energy absorbed in the rupture can be calculated from the initial and final missile velocities since

$$E \text{ absorbed} = \frac{1}{2} m (v_1^2 - v_2^2)$$

where v_1 is the missile striking velocity and v_2 is the residual missile velocity after the webbing has been broken. The initial velocity can be de-

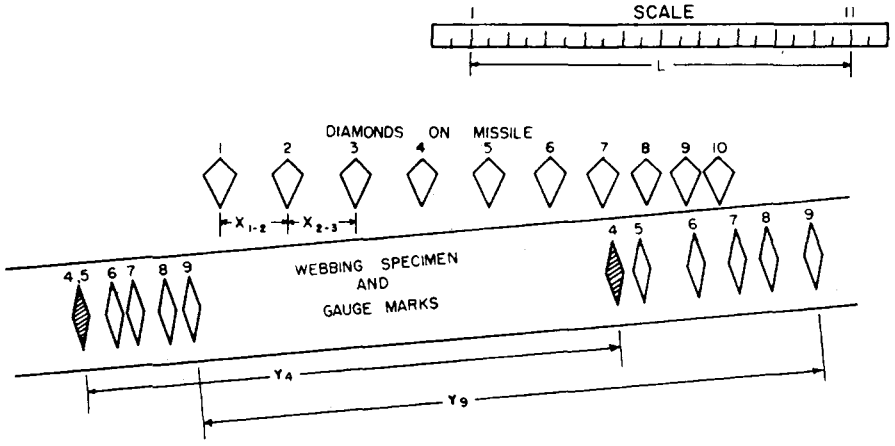

Fig. 9. Schematic diagram of shot No. 141.

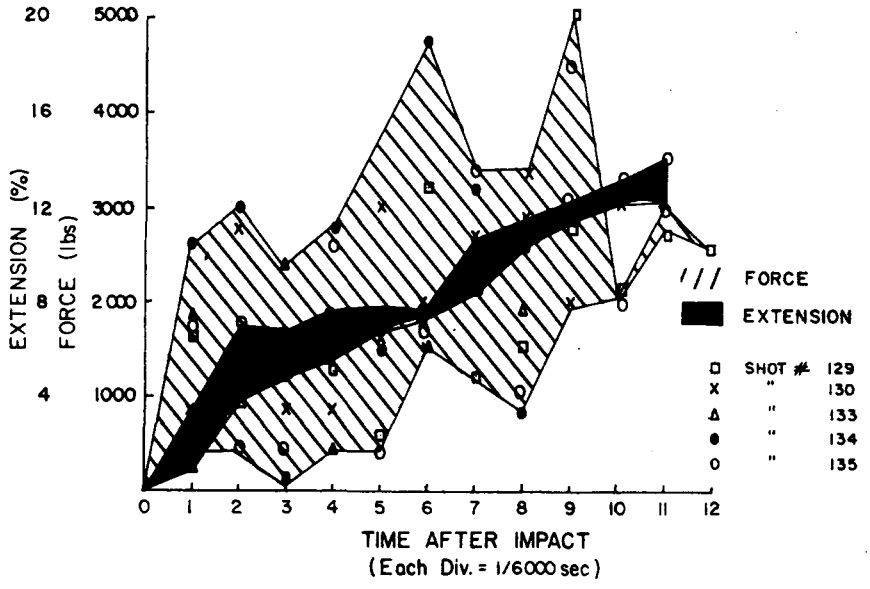

Fig. 10. Force, extension-time curves type WN 1512 webbing at 200 ft./sec.

termined either from the photograph of the impact since several pictures are always taken before the missile actually strikes the specimen or from the displacement of the first pendulum as described earlier.

DISCUSSION OF RESULTS

Figures 10, 11, and 12 illustrate the type of results obtained from the photographic measurements. Each of these plots is a composite force-extension versus time curve for a 1 in. nylon webbing, WN 1512, whose Instron breaking strength averages 6000 lb. with corresponding extension of 14%. Figure 10 is typical of the results obtained from the impact studies. The force-time curve is constructed from five missile firings at the webbing under study. It is shown as an envelope rather than an average curve since it is felt that this type of presentation most accurately depicts the type of behavior which actually exists under impact. The response of the specimen to the initial impact due to variations in clamping is such that in the first

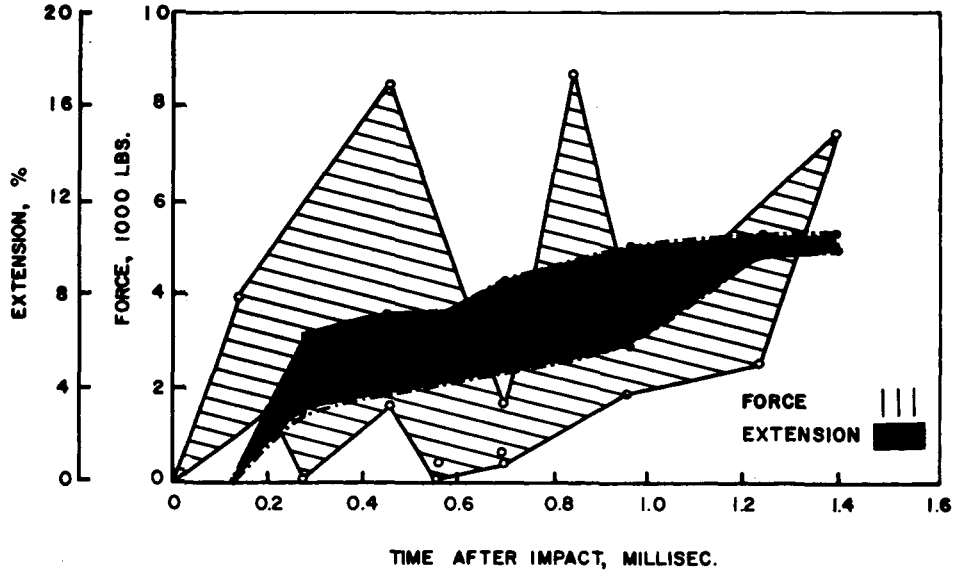

Fig. 11. Force, extension-time curves WN 1512 webbing at 400 ft./sec.

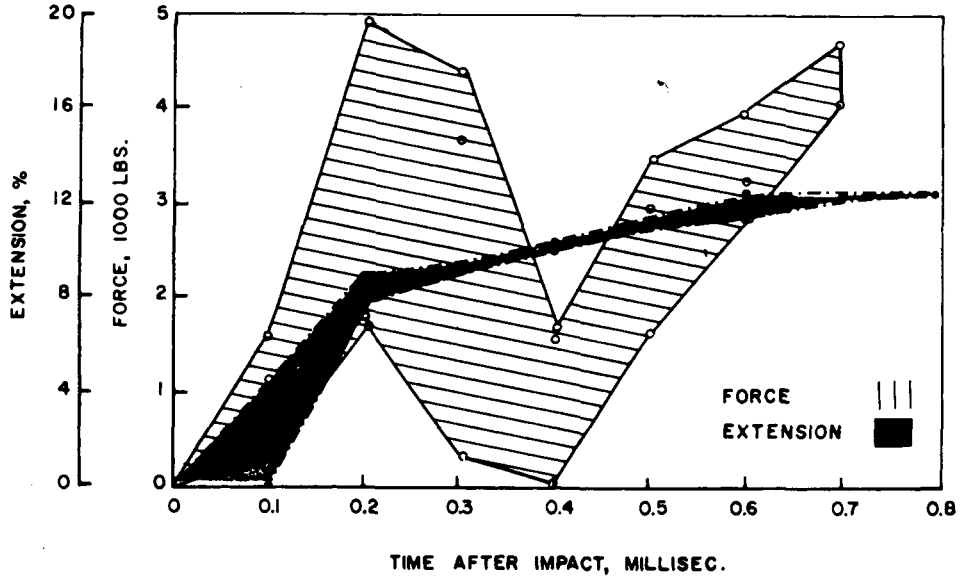

Fig. 12. Force, extension-time curves WN 1512 webbing at 700 ft./sec.

1/6000th of a second a force of 500 to 2500 lb. can be recorded from the missile deceleration. If the sample is initially tightly pulled around the capstan then a more rapid load buildup will occur than if the mounting load is rather light. On the Instron it is possible to measure this applied preload and maintain it from sample to sample. This is not as easily accomplished under impact. The overall time of test prior to rupture from Figure 10 would be approximately 1/700th of a second during which time it appears that the force exerted on the missile by the webbing rises and falls. If, for example, a line is drawn through the solid points (shot No. 134) it can be seen that the measured force progresses from 2700 to 3000 to 2800 to 1500 to 4700 lb. in 1/1000th of a second and then declines, apparently after rupture. Other individual points may be examined in similar fashion. While it must be conceded that some variability in force measurement can exist due to precision missile displacement variations it does not seem possible that variations in adjacent force measurements of the magnitude found can be explained from this fact alone.

As a matter of fact, the type of behavior noted can be explained from a theoretical consideration of the propagation of strain waves within a material under impact. Such an interpretation has been included in the Appendix. Briefly what is discussed is that the type of behavior noted can be explained in terms of wave theory. If a material is rapidly loaded at one end then a strain wave is transmitted along the specimen to the clamped end. At this point the wave is reflected (the extent of the reflection depends upon the type of grip) and begins to return toward the point of impact. A subsequent wave, however, has been generated at the contact end and this second pulse intercepts the returning one causing a further modification in its intensity. If the strain wave were reflected from a rigid boundary (a flat grip) then a rapid buildup could occur. The capstan grips are considered as a viscous boundary. The reflection which occurs is damped considerably, so that a rapid strain buildup does not always occur. A theoretical curve was constructed based upon these conclusions and compared with the experimental points determined for a particular test. Good correlation was shown.

Force pulses are known to travel in a similar manner and at speeds in excess of 5000 ft./sec. At these speeds and considering the impact velocity range under study it seems reasonable to postulate that force-wave reflections could easily be responsible for the apparently variable force-time curves.

Figures 11 and 12 illustrate the behavior of WN 1512 webbing when impacted at 400 and 700 ft./sec. Here the variations in forces appear even greater than at the lower speed. Strain variations are not as evident. One of the experimental difficulties can be mentioned here. In order to observe the complete behavior of the specimen under impact the time between light flashes can be varied. At high impact velocities the time between flashes

TABLE I
Maximum Measured Impact Forces and Extensions of Various Nylon Webbings Compared with Their Static or Slow Speed Behaviors

		Force, lb. at:				Extension, % at:		
Webbing type	Instron	200 ft./sec.	500 ft./sec.	700 ft./sec.	Instron	200 ft./sec.	500 ft./sec.	700 ft./sec.
WN 1505	4,000	3,650	2,470	5,300	18.0	18.2	14.0	20.2
WN 1512	6,000	4,925	8,640	4,900	14.0	14.0	10.9	12.5
WN 1509	9,100	7,550	8,300	6,400	19.0	18.1	13.6	14.4
Type XX	10,400	7,050	12,000	7,200	20.0	14.4	12.6	15.6

must be shortened since the overall time of test is reduced. If the time between flashes is too great then it is possible for the forces on the webbing to have built up and declined during the period when the light was out. If extremely short pulse times are used then the complete rupturing of a specimen cannot be obtained on one photographic negative. This difficulty can be remedied by the insertion of more discharge units into the multiflash system. Doubling the number of discharge units would effectively allow for a shortening of the time between pictures while keeping the overall exposure time constant. High speed motion picture cameras of the rotating drum type (framing rates in excess of 25,000 frames/sec.) are also being considered.

Table I is a summary of the maximum measured forces and extentions of various nylon webbings when compared with values measured on an Instron. Results indicate the forces and extensions measured under impact are generally close to the values obtained from the static tests. If endpoints alone are considered it could be postulated that the impact energy of the various webbings should be similar to that obtained from the area under the Instron curve. This is not always so as can be seen from Table II.

TABLE II
Comparison between Impact and Static Energy Absorption (ft.-lb.) of Various Parachute Components
(Values normalized to common 56-in. gage length)

	Instron	At 200 ft./sec.	At 500 ft./sec.	At 700 ft./sec.
Nylon Control Webbings				
WN 1505	895	812	1835	1783
WN 1512	1190	1469	2258	1694
WN 1509	2270	2976	5335	5151
Type XX	2270	4397	6269	5267
8 in. Overlap Splices Made from Nylon Control Webbings				
WN 1505	1057	1864	1948	1723
WN 1512	1232	2013	2960	1822
WN 1509	1802	2370	4673	2520
Type XX	2120	4703	5858	5042

Impact energy absorption of various materials, as shown in Table II, is determined mechanically rather than photographically as described earlier.

From the displacements of the pendulums it is possible to measure the energy absorbed in breaking the specimen. The energy measured from the area under the static stress-strain curve can be normalized to the impact specimen length so that a direct comparison between impact and static energy can be made. Impact energy as measured is an indication of the shape of the stress-strain curve of the material under impact. If the rupture stress and strain have not changed a great deal from the static values, then the curve shape must be different if the energy (area under the curve) is different. This is illustrated by Figure 13. If the static curve is shown as a straight line A then the area under the curve would be essentially that of a triangle or: $E = {}^1/_2 \times \epsilon$.

If the impact energy is double the static and the endpoints are the same, then the impact stress-strain curve at 500 and 700 ft./sec. would be similar

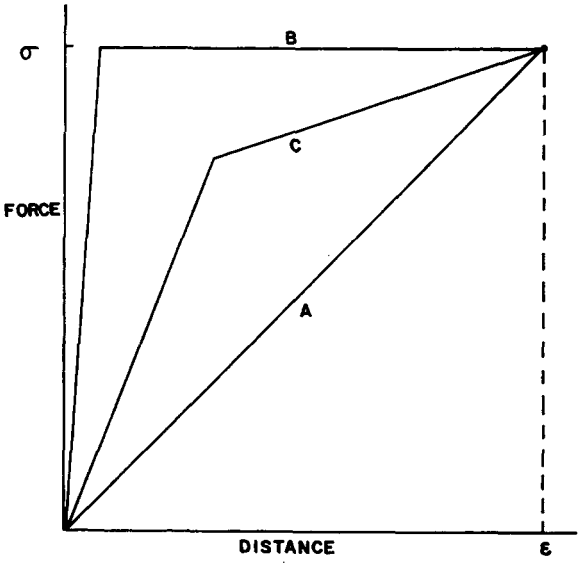

Fig. 13. Schematic force-distance diagram.

to curve B, or essentially that of a rectangle $E = \sigma \times E$.

At 200 ft./sec. the impact curve would be somewhere between curves A and B (curve C) and the area under the curve would be somewhere between the areas under curves A and B.

At least two important conclusions can be drawn from the results shown in Table II. The first is that the impact energies of the nylon control webbings and joints made therefrom (kinetic + strain) are always greater than the static values. The second is that the overlap splices made from the nylon control webbings appear to be highly efficient joints. The energy levels of the joints are generally equivalent to those of the control webbings. The exception to this is the WN 1509 overlap whose performance at the 700 ft./sec. level is 50% less than the control webbing at the same velocity. In general, however, the splices themselves never failed under impact. The break always occurred either at the missile contact point or at the capstan grip depending upon the striking velocity.

APPENDIX. THEORETICAL INTERPRETATION OF STRAIN-TIME CURVES*

The strain versus time curves can be explained, but not predicted, by assuming that the webbing has a linear stress-strain curve and that the capstan exerts a purely viscous force on the webbing.

Equating the acceleration of an element of webbing to the force per unit mass exerted on it gives the wave equation:

$$d^2w/dt^2 = (E/\rho)d^2w/dx^2 = c^2\, d^2w/dx^2 \quad \text{(A1)}$$

where $w(x, t)$ is the longitudinal displacement of the webbing at point x and time t, E is Young's modulus for the webbing in units of force, and ρ is its mass per unit length. If E is in units of stress, then ρ is in mass per unit volume. The general solution of eq. (A1) is:

$$w(x, t) = f(ct + x) + F(ct - x)$$

where f and F are arbitrary functions to be determined by the boundary conditions. The boundary condition at the capstan ($x = 0$) is

$$\text{Force} = E(dw/dx) = a(dw/dt) \quad \text{(A2)}$$

where a is the coefficient of viscosity relating force and velocity. The a is not measured and must be determined from experimental results. Plugging the general solution into eq. (A2) gives

$$(dw/dx)_{x=0} = f'(ct) - F'(ct)$$

$$f'(y) = df(y)/dy$$

where

$$(dw/dt)_{x=0} = cf'(ct) + cF'(ct)$$

$$(E + ac)F'(ct) = (E - ac)f'(ct)$$

Integration gives:

$$F(ct) = Rf(ct) \quad \text{or} \quad F(ct - x) = Rf(ct - x)$$

where $R = (E - ac)/(E + ac) - R$ may be considered a reflection coefficient, so that

$$w = f(ct + x) + Rf(ct - x) \quad \text{(A3)}$$

The boundary condition at $x = s$ (the length of the webbing) is the equation of motion of the missile which is given in the following form (from Love, A. E. H., *A Treatise on the Mathematical Theory of Elasticity*, Dover, New York, 1944, p. 431):

$$ms\, d^2w/dt^2 = -c^2\, dw/dx \quad \text{(A4)}$$

where m is the missile mass/webbing mass. Plugging expression (A3) into eq. (A4) gives:

$$(d^2w/dt^2)_{x=s} = c^2f''(ct + s) + c^2Rf''(ct - s)$$

$$(dw/dx)_{x=s} = f'(ct + s) - Rf'(ct - s)$$

These expressions give a "continuing equation"

$$f''(y) + (1/ms)f'(y) = -R[f''(y - 2s) - (1/ms)f'(y - 2s)] \quad \text{(A5)}$$

which allows a solution to be found at any time in terms of the solution at a previous time. Using eq. (5) and the fact that $w = 0$ for t less than 0 and the fact that w and dw/dt are continuous gives the following expressions for $w(x, t)$:

$ct + x < s$

$$w = 0$$

$ct - x < s, \quad ct + x > s$

$$w = (msV/c)[1 - \exp\{-(ct + x - s)/ms\}]$$

where V = impact speed

$ct + x < 3s, \quad ct - x > s$

$$w = (msV/c)([1 - \exp\{-(ct + x - s)/ms\}] + R[1 - \exp\{-(ct - x - s)/ms\}])$$

* Prepared by Stephen D. Weiner, currently a graduate student at Massachusetts Institute of Technology.

$$ct - x < 3s, \quad ct + x > 3s$$

$$w = (msV/c)([1 - \exp\{-(ct + x - s)/ms\}] + R[1 - \exp\{-(ct - x - s)/ms\}] + R[1 - \{1 + (2/ms)(ct + x - 3s)\} \exp\{-(ct + x - 3s)/ms\}]) \quad \text{(A6)}$$

$$ct + x < 5s, \quad ct - x > 3s$$

$$w = (msV/c)([1 - \exp\{-(ct + x - s)/ms)\}] + R[1 - \exp\{-(ct - x - s)/ms\}] + R[1 - \{1 + (2/ms)(ct + x - 3s)\} \exp\{-(ct + x - 3s)/ms\}] + RR'[1 - \{1 + (2/ms)(ct - x - 3s)\} \exp\{-(ct - x - 3s)/ms\}])$$

where R' is the value of R when $ct = 3s$.

The strain ϵ in a section of webbing between x_1 and x_2 at time t is given by

$$\epsilon(t) = [w(x_2, t) - w(x_1, t)]/(x_2 - x_1) \quad \text{(A7)}$$

In terms of this theory, a fairly typical test can be interpreted as in Figure 14. From A to B the initial strain pulse is propagating from the first mark on the webbing to the second and the total strain increases almost linearly as more of the section is strained. From B to C the wave front has passed the second mark and the strain decreases slightly because of the slowing of the missile. The wave is partly reflected at the capstan and from C to D the reflected pulse is propagating from the second mark to the first. Depending on the value of a, the coefficient of viscosity at the capstan R (reflection coefficient) can range from -1 to $+1$. For a completely rigid boundary, $R = -1$ and the strain at D will be almost twice the strain at B.

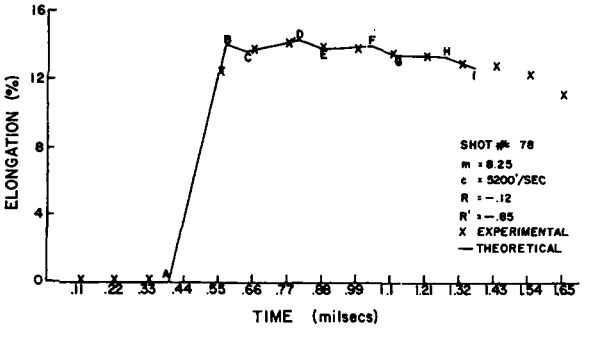

Fig. 14. Strain of 10 in. section of webbing versus time.

For a free boundary, $R = +1$, and the strain at D will go to zero. From D to E the strain decreases. It decreases more rapidly than from B to C because it is the sum of the decreases from two pulses, the initial and the reflected ones. The missile acts as a rigid boundary with $R = -1$ so the reflected wave is completely reflected, changing only slightly in shape. From E to F this pulse propagates from the first to the second mark. From F to G the strain decreases again. The wave that was just reflected at the missile, is now reflected at the capstan. The value of R has changed since the last reflection because of a change in the coefficient of viscosity. This change is expected physically because in some cases the webbing fuses on itself inside the capstan, increasing the viscosity, and in other cases, the webbing breaks inside the capstan, decreasing the viscosity. From G to H this reflected pulse propagates from the second to the first mark. From H to I the strain again decreases. The theoretical curve has not as yet been calculated beyond point I. Points will be calculated beyond point I and compared to the experimental data at a later date. In addition there are complications introduced by the fact that a wave is propagated inside the capstan which, when reflected, would after point I, affect the strain in the 10 in. section. The next step in the theoretical calculations will be to consider the wave inside the capstan in order to continue the curve and to determine the boundary condition at the capstan more realistically. There are several other corrections which would change the curve slightly. The webbing, while it is perfectly elastic, returning to its original length after testing, is not exactly linear in its stress-strain behavior. However, materials generally become more linear as strain rate is increased (Meredith, R., *The Mechanical Properties of Textile Fibers*, Interscience New York–London, 1956, p. 274) so the error introduced by assuming linear behavior is not very large. As time increases, the webbing is pulled out of the capstan increasing s, increasing the webbing mass thus decreasing m. Thus ms remains constant although other parameters such as c may change. A change in c would also change the magnitude of the strain but as the data are suitable for the constant value of C, the change in c is probably small.

A force on missile versus time curve can be found by finding $M(d^2w/dt^2)_{x=s}$, where M is the missile mass. This force agrees with experiment within experimental error, but as this error may be as much as 20%, the agreement is not conclusive.

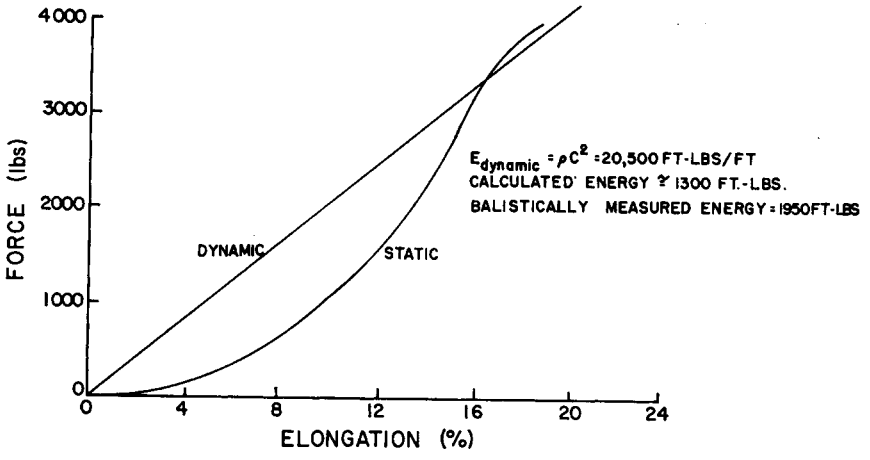

Fig. 15. Static and dynamic stress-strain curves.

From the relation $E = \rho c^2$ for the linear model of the webbing used in calculations, a dynamic stress-strain curve can be found. This curve approximates the static curve as shown in Figure 15. The accuracy of this curve depends on the accuracy of c. The value of c can be determined directly from the photograph to within 30%. It can be found from the relation $c = V/\epsilon$ to within 9%. By fitting a theoretical curve to the experimental results, c can be determined to within about 3% but this procedure is very time-consuming and was not done in many cases. By measuring the area under the dynamic stress-strain curve corresponding to the measured strain, an approximate value of energy absorbed can be found. This value should be less than that measured ballistically since it includes only elastic energy while energy is also absorbed as heat at the capstan. In some cases when the webbing breaks at one capstan, the webbing has kinetic energy which is not delivered to the second pendulum and is measured as part of the energy absorbed. Since the strain is known over a limited time and it cannot be determined whether this time includes the time of break, the rupture strain and thus the energy to break cannot be determined with much accuracy. Measurements of energy are actually made ballistically as described above and the fact that calculated values are of the same order of magnitude serves as a check on the theory. The values of modulus and energy should be affected by deviations from linearity much more than are values of strain as the results indicate.

The most important result of the theory is that the strain and thus the stress in the webbing can exceed that produced by the initial impact alone. With a perfectly rigid capstan boundary, the strain at B would be that produced by the initial impact. The strain at D would be two times that at B, the strain at F would be three times that at B, and the strain at H would be four times that at B. The force at any time, the time taken to break the webbing, and thus the energy absorbed depend greatly on the characteristics of the boundary.

Synopsis

A machine has been designed and constructed which is capable of evaluating high strength parachute components in the laboratory at impact speeds ranging from 200–750 ft./sec. The system consists mainly of a device for propelling various masses with photographic instrumentation for observing the impact. Measurement of missile deceleration gives applied force. Extension is measured for changes in gage marks on the test specimen. Energy absorbed can be calculated from the displacement of two ballistic pendulums. Results reveal that at impact speeds force and strain waves are generated within the material which cause rapid changes in the forces measured. A theory has been proposed to explain this behavior. Energy measurements indicate a potential change in the stress-strain curve of nylon webbings and joints during impact. Improvements in energy absorption result.

Résumé

On a dessiné et construit une machine capable d'évaluer les composants des forces de choc d'un parachutage dans le laboratoire à des vitesses de choc chiffrant de 200 à 750 pieds par seconde. Le système consiste principalement en un stratagème destiné à propulser des masses variables et à observer l'impact grâce à un appareillage photographique. La mesure de la décélération des projectiles donne la force appliquée. On mesure l'extension à partir des variations des jauges sur l'échantillon étalon. On peut calculer l'énergie adsorbée à partir du déplacement de deux pendules balistiques. Les résultats révèlent qu'à l'impact il se forme des forces de vitesse et des ondes de tension à l'intérieur du matériel, ce qui cause des variations rapides dans les forces

mesurées. On propose une théorie pour expliquer ce comportment. Des mesures de l'énergie indiquent une variation de potentiel dans la courbe force-tension des sangles et des joints de nylon pendant l'impact. Il en résulte des améliorations dans l'adsorption d'énergie.

Zusammenfassung

Ein Apparat zur Testung von Fallschirmbestandteilen hoher Festigkeit im Laboratorium bei Schlaggeschwindigkeiten von 200 bis 750 Fuss per Sekunde wurde entworfen und gebaut. Der Hauptbestandteil des Systems ist eine Vorrichtung zum Antrieb verschiedener Massen mit einer photographischen Ausrüstung zur Beobachtung des Schlages. Die Messung der Geschwindigkeitsabnahme des Wurfkörpers liefert die angewendete Kraft. Die Dehnung wird aus der Verschiebung von Massstabsmarken auf der Testprobe bestimmt. Die absorbierte Energie kann aus der Verrückung zweier ballistischer Pendel berechnet werden. Die Ergebnisse zeigen, dass bei Schlaggeschwindigkeiten Kraft- und Verformungswellen in der Probe entstehen, die schnelle Veränderungen der gemessenen Kräfte verursachen. Eine Theorie zur Erklärung dieses Verhaltens wird angegeben. Energiemessungen lassen eine Potentialänderung in der Spannungsdehnungskurve von Nylongurten und Verbindungsstücken während des Schlages erkennen. Daraus ergibt sich eine verbesserte Energieabsorption.

Discussion

Question: You have shown that there were rather drastic changes in force during your tests. Is it possible that owing to the nature of the capstan jaw some extension occurred on that portion of the test specimen which is wrapped around the jaw?

Answer (Mr. Coskren): Yes. On a standard tensile tester such as the Instron, when a webbing is mounted in capstan jaws for testing, the specimens are generally preloaded by a lowering of the crosshead so that the sample is tight on the jaws. On the impact tester, when the sample is mounted horizontally, it is pulled tight manually. With this technique it is possible that there is still some initial rearrangement or extension of the webbing around the jaw prior to the actual load buildup during the test.

Question: Are your energy calculations from the ballistic pendulums based upon perfect elastic collisions?

Answer (Mr. Coskren): Yes.

Question: This may be part of the reason for the higher energies you have shown.

Answer (Mr. Coskren): That is true. In fact, the energy given in Table II is the sum of all energy absorbed by the specimen—strain, kinetic, and heat.

Answer (Dr. Morgan): I think what Mr. Coskren failed to mention is that we are not very happy with the force measurements. When you do a double differentiation and start with a 1% error in your displacement measurement, large errors can occur in calculating forces, as you know, so that you may think at first that these cyclical high- and low-force values are due to strain wave reflections. However, if you calculate the strain wave velocity you find that these fluctuations can be due largely to slight variations in measurement and not to the actual behavior of the test specimen.

The load sometimes started to build up before any strain was noted in the specimen. This is indicative of the time it takes the stress to travel down the sample. The stress wave travels at about 5000 ft./sec. in these webbings, as measured from the photographs. In the expression $E = v/c$, the c, which is the 14% strain velocity at 800 ft./sec. impact velocity, would be of the same order of magnitude as the 5000-ft./sec. value measured; thus, while there is a poor check on the force calculations, this technique does give good checks on strain wave theory.

The other problem in the measurement of force is that it is being measured only at the impacted end. The sample doesn't always break where it is hit, so that the maximum force could be developed at the fixed end and never be measured.

END OF SYMPOSIUM